The effect of branched structures of alkyl groups on tissue adhesiveness and biocompatibility of alkyl groups-modified Alaska pollock gelatin-based adhesives

Satsuki Minamisakamoto[1,2], Hiyori Komatsu[1,2], Shiharu Watanabe[2], Shima Ito[1,2], Hatsune Nishino[2,3], Tetsushi Taguchi[1,2]*

[1]Graduate School of Science and Technology, Degree Programs in Pure and Applied Sciences, University of Tsukuba, 1-1-1 Tennodai, Tsukuba, Ibaraki 305-8577, Japan

[2]Biomaterials field, Research Center for Macromolecules and Biomaterials, National Institute for Materials Science, 1-1 Namiki, Tsukuba, Ibaraki 305-0044, Japan

[3]College of Engineering Science, School of Science and Engineering, University of Tsukuba, 1-1-1 Tennodai, Tsukuba, Ibaraki 305-8577, Japan

Correspondence and requests for materials should be addressed to T. Taguchi. (email: TAGUCHI.Tetsushi@nims.go.jp)

Abstract

Tissue adhesives are widely used to prevent air leakage from the lungs and bleeding from vascular anastomoses. However, currently used tissue adhesives still face challenges with either tissue adhesion or biocompatibility. We previously reported tissue adhesives composed of straight alkyl group-modified Alaska pollock gelatin (ApGltn) and pentaerythritol poly (ethylene glycol) ether tetrasuccinimidyl glutarate (4S-PEG). The developed adhesives have sufficient tissue adhesive strength and biocompatibility for biomedical applications; however, the effect of the branched structures of the alkyl groups on these functions has not yet been clarified. In this study, we evaluated the tissue adhesiveness and biocompatibility of three tissue adhesives based on straight/branched alkyl group-modified ApGltns and 4S-PEG. The results showed that branched alkyl-group-modified ApGltns-based adhesives had higher tissue adhesion strength than straight alkyl-ApGltn. Furthermore, the burst strength of the branched alkyl group-modified ApGltn-based adhesives 2-fold higher compared to commercial Fibrin. In addition, they were completely biodegraded in rat subcutaneous tissue within 56 days without causing severe inflammation.

Keywords: in situ hydrogel; tissue adhesion; Alaska pollock-derived gelatin; hydrophobic interaction.

1. Introduction

Tissue adhesives are widely used in clinical practice to prevent air leakage from the lungs or oozing from vascular anatomic sites. Various tissue adhesives, such as cyanoacrylate, albumin with aldehyde, and fibrin glue, have been developed to close or seal wounds after surgical operations [1]. Cyanoacrylate adhesives exhibit superior adhesive strength and the ability to bond to wet tissues via water-mediated polymerization [2]. Although it has been mainly used for skin adhesion, the release of formaldehyde through the degradation process of cyanoacrylate adhesives is toxic to the body [3]. Other adhesive made from bovine serum albumin and glutaraldehyde as crosslinkers have high adhesive strength owing to Schiff base formation between the primary amine of albumin and glutaraldehyde [4]; however, the release of unreacted glutaraldehyde from cured adhesives also shows toxicity [5]. Therefore, fibrin glue is commonly used post-operatively. It is mainly composed of human blood-derived fibrinogen and thrombin [1, 2] and shows superior biocompatibility; however, its adhesiveness is weak compared to that of cyanoacrylate and albumin-glutaraldehyde adhesives because of its weak interaction with biological tissues. Therefore, commercial tissue adhesives face challenges in terms of strong tissue adhesion and superior biocompatibility. Some functional groups such as N-Hydroxy succinimide (NHS) ester, aldehyde, and catechol have been introduced to the hydrogel

for high adhesion to tissue, removing the hydration layer on the tissue surface and building connectivity between the adhesive and tissue through covalent bonds to address these issues [6, 7]. It has also been reported that double network hydrogels, tetra-PEG gels, slide-ring gels and nanocomposite hydrogels have a crosslinking style for greater bulk strength [8-11]. We have previously developed hydrophobic-modified Alaska pollock-derived gelatin (ApGltn)-based tissue adhesives [12, 13]. ApGltn has a low sol-gel transition temperature for dissolution at room temperature, enabling dissolution in the freeze-dried state without heating. Using ApGltn as a base polymer, we designed tissue adhesives made from straight alkyl group-modified ApGltns and pentaerythritol poly (ethylene glycol) ether tetrasuccinimidyl glutarate (4S-PEG) and demonstrated their excellent tissue adhesiveness and biocompatibility. However, the effects of branched alkyl groups structures on the adhesive strength and biocompatibility of tissue adhesives have not yet been elucidated. It is known that the shorter the main-chain length of an alkyl group, the lower the enthalpy and entropy of melting when the number of carbons is the same [14, 15]. In this study, we synthesized three straight/branched alkyl group-modified ApGltns and evaluated their tissue adhesiveness and biocompatibility of tissue adhesives based on the alkyl group-modified ApGltns and 4S-PEG (**Figure 1**). It is anticipated that tissue adhesives based on branched alkyl group-modified ApGltns will exhibit superior

handling and higher tissue adhesiveness owing to their improved mobility or interpenetration resulting from their lower hydrophobicity and viscosity [16].

2. Materials and Methods

2.1. Materials

ApGltn was purchased from Nitta Gelatin, Inc. (Osaka, Japan). Dulbecco's Phosphate-Buffered Saline (D-PBS), dimethyl sulfoxide (DMSO), triethylamine (TEA), 2,4,6-trinitrobenzensulfonic acid (TNBS), 6 N-hydrochloric acid (HCl), boric acid, potassium chloride, sodium hydroxide, phosphoric acid, sodium dihydrogen phosphate, bovine serum albumin (BSA), paraformaldehyde, 4',6-diamidino-2-phenylindole (DAPI) and 10% formalin neutral buffer solution were purchased from Wako Pure Chemical Industries, Ltd (Osaka, Japan). n-Octanal and 2-ethylhexanal were purchased from Tokyo Chemical Industry Co., Ltd. (Tokyo, Japan). 2-propyl valeraldehyde was kindly donated by Santa Cruz Biotechnology Inc. (Dallas, TX, USA). 2-Picoline borane was purchased from Junsei Chemical Co. Ltd. (Tokyo, Japan). DMSO-d_6, Roswell Park Memorial Institute (RPMI) medium, and fetal bovine serum (FBS)-FITC/Phalloidin were purchased from Sigma-Aldrich Co., LLC (St. Louis, MO, USA). Penicillin/streptomycin was purchased from Thermo Fisher Scientific (Tokyo, Japan). Triton-X was purchased from

Cayman Chemical (Ann Arbor, MI, USA). TrypLE Express was purchased from Life Technologies (Grand Island, NY, USA). Collagenase and Water-soluble tetrazolium (WST) -8 were purchased from NACALAI TESQUE, INC. (Kyoto, Japan). The mouse fibroblast-like cell line (L929) was purchased from RIKEN (Saitama, Japan). 99.5% Ethanol was purchased from Kishida Chemical Co., LTD (Osaka, Japan). 4S-PEG was purchased from NOF Co., Ltd. (Tokyo, Japan). Beriplast-P (Fibrin) was purchased from CSL Behring (Tokyo, Japan). Collagen casing was purchased from Nippi, Incorporated (Tokyo, Japan). Saline was purchased from Otsuka Pharmaceutical Co. Ltd. (Tokyo, Japan). Rats (Wistar, male, 6 weeks old) were purchased from Jackson Laboratory Japan (Kanagawa, Japan).

2.2. Synthesis of C8-ApGltns

Three straight/branched alkyl group-modified ApGltns (C8-ApGltns) were synthesized using a previously reported [17, 18]. We employed n-octyl group (straight), 2-ethylhexyl group (branched), and 2-propylpentyl group (branched), which have eight carbons, as the straight/branched alkyl groups. Straight/branched alkyl groups-modified ApGltns were synthesized by reductive amination of the amino groups of the original ApGltn (Org-ApGltn) with alkyl aldehydes (**Figure 1**). Briefly, Org-ApGltn was dissolved in

water/EtOH (50/50 (v/v)) mixed solvent to obtain a 15 w/v% solution at 50 °C. Alkyl aldehyde was then added to the solution and stirred for 1 h. After that, 2-picoline borane was added to the reaction solution and the mixture was stirred for 18 h at 50 °C. The resulting C8-ApGltns were re-precipitated in cold EtOH and washed three times with cold EtOH to remove unreacted alkyl aldehyde and 2-Picoline borane. The precipitates were then filtered and dried under reduced pressure for 2 days at room temperature.

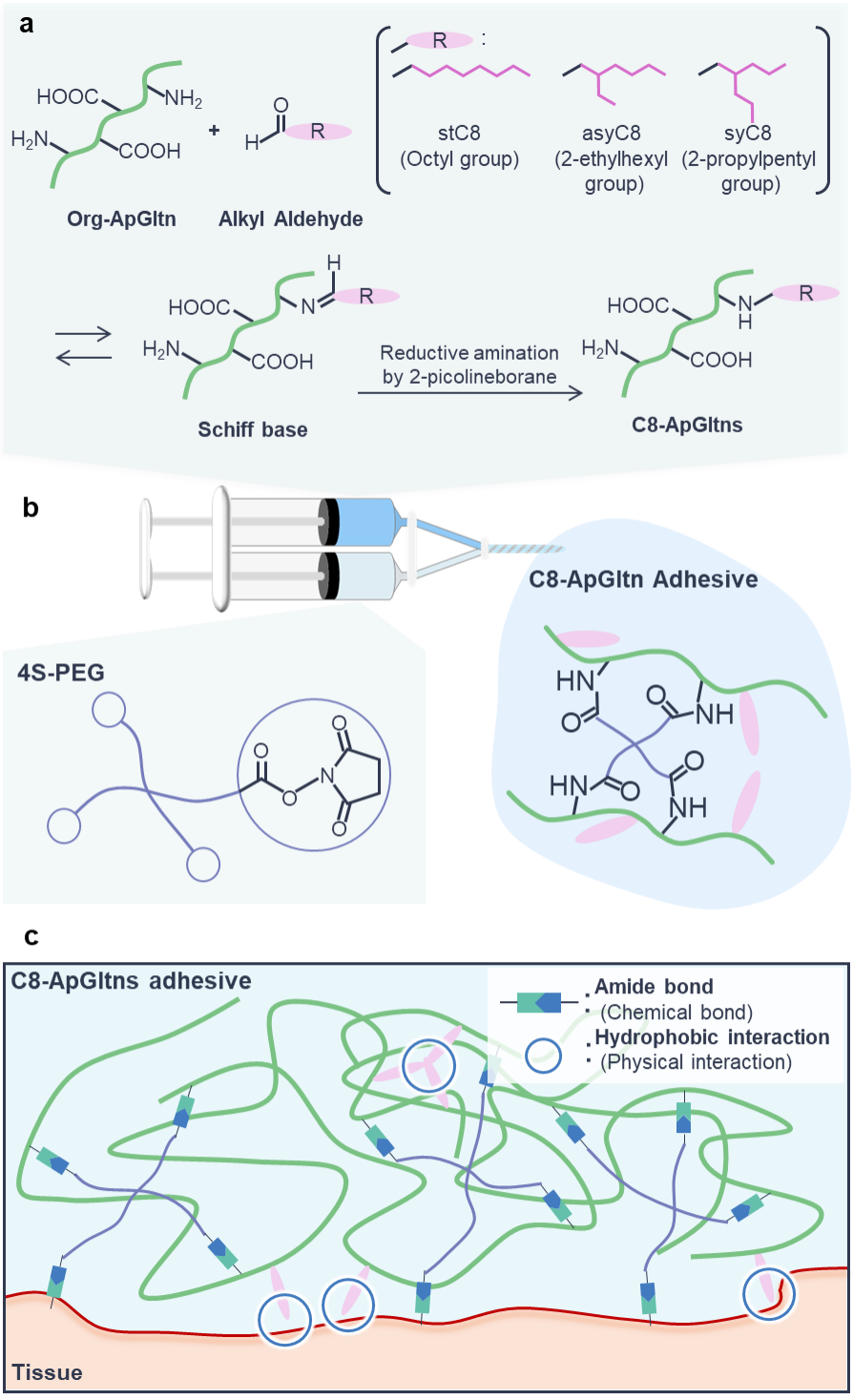

Figure 1. Application of C8-ApGltn adhesives to soft tissue. a) Synthesis of C8-ApGltns through Schiff base formation and reductive amination using straight/branched alkyl aldehydes. b) In situ crosslinking of C8-ApGltn with 4S-PEG. c) Adhesion mechanism of C8-ApGltn adhesives after application onto soft tissue.

2.3. *Characterization of C8-ApGltns*

The degree of modification of the resulting C8-ApGltns were determined based on the residual amino group content using TNBS, method, as reported previously [19, 20]. We prepared 0.1 w/v% each Org and C8-ApGltns solution using the water/DMSO (50/50 (v/v)) mixed solvent. 100 μL of each solution was dispensed to well plate (n=9) and added the 100 μL of TEA (0.1 v/v%) and TNBS (0.1w/v%) solution. After reaction at 37 °C for 2 h, DS was determined from the ratio of absorbance at 340 nm. Modification of the straight/branched alkyl groups was also confirmed using Fourier transform infrared spectroscopy (FT-IR) (ALPHA II; Bruker Japan K. K., Kanagawa, Japan) and proton nuclear magnetic resonance (^{1}H NMR) (ECZ400S; JEOL, Tokyo, Japan) in DMSO-d_6 containing 0.03 v/v% of tetramethylsilane (TMS) as a standard substance.

2.4. *Gelation time of C8-ApGltns adhesives*

C8-ApGltns adhesives were prepared by mixing 4S-PEG (40 mol% of the amino groups of Org-ApGltn in 0.01 M phosphate buffer, pH 4) with Org-ApGltn or straight/branched alkyl groups-modified ApGltns solutions at 1:1 using a double syringe (Bethel Co., Ltd., Ibaraki, Japan) to prepared adhesive hydrogels in situ [21]. The solvent of all ApGltns solutions was borate buffer (0.075 M, pH 9.5). The gelation time of Org and C8-ApGltns

adhesives were measured according to a previously reported [22, 23]. Briefly, 500 μL of Org or C8-ApGltns solutions were poured into a 9 mL screw tube and stirred with an 18 mm stirrer at 290 rpm and 37 °C. The gelation time was defined as the time until the rotation of the stirring bar was hindered by the gelatin after addition of 500 μL of 4S-PEG solution (n = 3–4).

2.5. *Swelling ratio*

The swelling ratio of the C8-ApGltn adhesives was measured by immersing Org or C8-ApGltns adhesive hydrogels in D-PBS, as previously reported [13, 24]. Briefly, Org-ApGltn or C8-ApGltn/4S-PEG mixed solutions were poured into a silicone mold to prepare disks 10 mm in diameter and 1 mm thick. The disks were immersed into 50 mL D-PBS at 37 °C in centrifuge tubes and weighed after immersion for various periods (W_s) [13]. The D-PBS in the centrifuge tube was replaced each time. The swollen adhesives were then immersed in 50 mL of ultrapure water three times every 30 min to remove salt and freeze-dried for 24 h. Finally, the freeze-dried adhesives were weighed (W_d) to determine the swelling ratio using the following equation:

$$Swelling\ \ ratio = \frac{W_s - W_d}{W_d}$$

2.6. Rheological measurement

Rheological measurements of the Org/stC8/asyC8/syC8-ApGltn hydrogels were performed using a rheometer (MCR301; Anton Paar, Graz, Austria) with a PP10 parallel plate (10 mm) [17]. Adhesive (30 μL) was applied to the stage of the rheometer at 37 °C and sandwiched between plates separated by a 1 mm gap. After removing the excess adhesive from the PP10 plate, the adhesive was left for 10 min to allow sufficient gelation. First, shear strain was measured to determine the linear viscoelastic (LVE) region of the cured adhesive hydrogels. The storage modulus (G') and loss modulus (G") were measured at an angular frequency of 10 rad/s with changing shear strains ranging from 0.01% to 100%. Then, an angular frequency from 1 to 100 rad/s was measured at strain amplitude within the LVE region at 37 °C. The viscosities of Org and C8-ApGltns solutions at room temperature were measured using a viscometer (VM-10A; SEKONIC, Tokyo, Japan).

2.7. Tensile strength measurement

The tensile strengths of Org and C8-ApGltns adhesive hydrogels were measured according to ASTM D412 [17]. Dumbbell-shaped adhesive hydrogels with a thickness of 1 mm were prepared for tensile strength measurements (**Figure S3a**). The tensile strength

was measured using a texture analyzer (TA.XTplusC Texture Analyzer; Stable Micro Systems, Surrey, UK) under fixed conditions (temperature: 25 °C, humidity: 60–70%, strain rate: 10 mm/min).

2.8. Burst strength measurements

The burst strengths of Org and C8-ApGltns adhesives were measured according to ASTM 2392-04 (**Figure S4**). Commercial Fibrin was also used as a control adhesive. The collagen casing was prepared by cutting it into a disk 35 mm in diameter with a hole of 3 mm in diameter at the center. Then, a silicone mold with a diameter of 35 mm and a thickness of 1 mm, with a hole 15 mm in diameter at the center, was placed on the surface of the collagen casing. Org and C8-ApGltn adhesives were used to seal the holes. After 10 min, a collagen casing with an adhesive was placed on the stage of the test system at 37 °C to measure the burst strength. Saline was poured through the bottom of the collagen casing at a flow rate of 2 mL/min. The burst strength for each condition was defined as the maximum burst strength at which the adhesive fractured or peeled off (**Figure 4b**) [25].

2.9. *In vitro enzymatic degradation test*

Disk-shaped adhesive hydrogels (6 mm in diameter, 1 mm in thickness) were immersed in 5 mL of 1.25 U/mL of collagenase in D-PBS To assess the in vitro biodegradability of Org or C8-ApGltns adhesive hydrogels, [12, 26]. After immersion for various periods, the adhesive hydrogels were placed in ultrapure water to remove salts and then freeze-dried (n = 3). The mass of the adhesive hydrogel was measured at each time point. W_0 and W_t indicate the mass of the freeze-dried adhesive hydrogels before and after immersion in the collagenase solution, respectively. Biodegradability was calculated using the following equation:

$$Weghit\ remaining\ (\%) = \frac{W_t}{W_0} \times 100$$

2.10. *Cytocompatibility*

The cytocompatibility of Org and C8-ApGtlns adhesives was evaluated according to ISO 10993-5 and 10993-12 [17]. Adhesive hydrogels with a mass extraction rate of 0.1 g/mL and surface extraction rate of 3 mm^2/mL were cut to prepare the extraction medium for each adhesive. Obtained samples were then immersed into RPMI medium for 24 h at 37 °C. For the evaluation of cytocompatibility, 1.0×10^4 fibroblasts (L929) were seeded into 20 wells in a 96-well plate and preincubated for 24 h at 37 °C. All media were removed and replaced with the extracted medium (n = 5). The RPMI medium without

samples was used as a control. The number of viable cells in each well was measured after incubation for 24 h using the WST-8. Before observing the cell morphology, the cells were fixed with 4% PFA for 15 min at 4 °C and washed twice with D-PBS. BSA (1% in D-PBS) was used for blocking to prevent non-specific binding of antibodies, and Triton-X (0.2% in D-PBS) was used for transparent processing. Actin filament was stained with 0.1% FITC/phalloidin at D-PBS and nuclear with 0.1% DAPI at D-PBS. The cell morphology was observed using a fluorescence microscope (BZ-X710; KEYENCE, Osaka, Japan).

2.11. Subcutaneous implantation

All animal experiments were approved by the Animal Experiment Committee of the National Institute for Materials Science (approval no. 79-2024-3). Disk-shaped adhesive hydrogels (thickness: 0.5 mm, diameter: 6 mm) were prepared and sterilized using UV irradiation for 15 min. The rats were then anesthetized by isoflurane inhalation, and a 1 cm incision was made at the back of each rat after shaving. The tissues around the adhesives were then excised, fixed with a neutral buffered 10% formalin solution, and stained with hematoxylin and eosin (HE) for histological observation.

2.12. Statistical analysis

Statistical analyses were performed using one-way or two-way ANOVA followed by Tukey's multiple comparison test. Statistical significance was set at $p < 0.05$.

3. Results and Discussion

3.1. Synthesis and characterization

C8-ApGltns (stC8/asyC8/syC8-ApGltns) with different alkyl structures and degrees of substitution (DS) were synthesized by reductive amination of alkyl aldehydes to the amino groups of Org-ApGltn. As shown in **Table 1**, stC8/asyC8/syC8-ApGltns were obtained at high yields (>80%); stC8/asyC8-ApGltns had low (approximately 10 mol%) (L), medium (approximately 30 mol%) (M), and high (approximately 45 mol%) (H) DS; and syC8-ApGltn had only low DS. There were 1.3 alkyl groups per Org-ApGltn molecule in stC8 (L). The FT-IR spectra revealed that the specific peaks corresponding to the N-H stretching vibration of the secondary amine (3,290 cm^{-1}) increased with an increase in DSs (**Figure 2a, b**). In addition, the specific peaks assigned to the C-H symmetric stretching vibration in CH_3 (2,880 cm^{-1}), C-H asymmetric stretching vibration in CH_2 (2,940 cm^{-1}), and CH_3 (2,960 cm^{-1}) indicated that alkyl groups were successfully introduced to Org-ApGltn. The ^1H NMR spectra revealed that the intensity of the stronger specific peaks of CH_3 and CH_2 at 0.85 and 1.24 ppm, respectively, increased with increasing DSs (**Figure 2c**). In addition, the peaks of stC8/syC8-ApGltn in the ^1H NMR spectra were sharper than those of asyC8-ApGltn because of the diverse proton environment of asyC8-ApGltn.

Table 1. Characteristics of C8-ApGltns with straight (stC8), asymmetric (asyC8) and symmetric (syC8) alkyl groups

Abbreviation	ApGltn (g)	Amino groups in ApGltn (μmol/g)	Theoretical DS (mol%)	DS (mol%)	Yield (%)
stC8 (L)	5	351	10.3	9.1	87.3
stC8 (L)	30	357	10	8.1	93.2
stC8 (M)	5	351	50	28.6	84.9
stC8 (H)	5	351	154	45.3	86.0
asyC8 (L)	5	351	10	9.4	88.0
asyC8 (L)	30	357	10	8.2	93.4
asyC8 (M)	5	351	40	30.5	85.8
asyC8 (H)	5	351	90	44.5	86.3
syC8 (L)	5	357	10	8.6	82.7

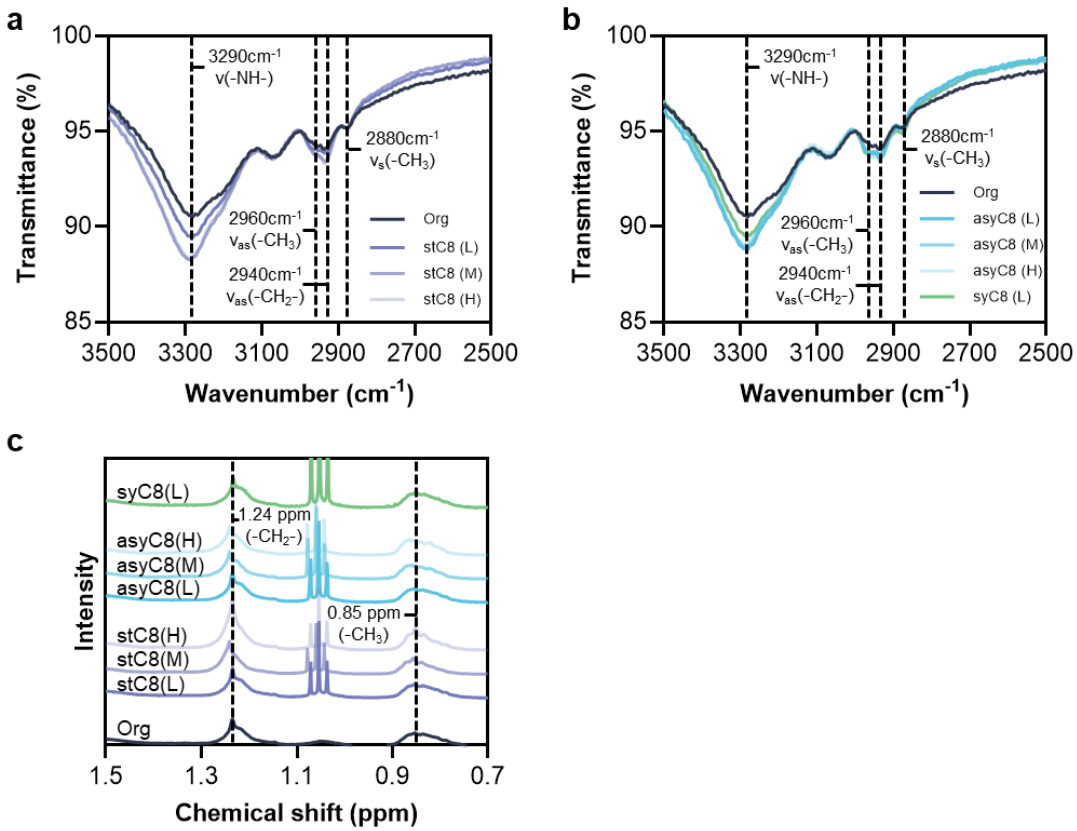

Figure 2. Characterization of C8-ApGltns. a) FT-IR spectra of stC8-ApGltns. b) FT-IR spectra of branched asyC8/syC8-ApGltns. c) ^{1}H NMR spectra of Org/stC8/asyC8/syC8-ApGtlns.

3.2. Gelation time

Gelation of the Org or C8-ApGltns adhesives proceeds by the nucleophilic attack of the amino groups of Org or C8-ApGltns on the carbonyl carbon of the active ester groups in 4S-PEG. **Figure 3a** shows the gelation time of Org and C8-ApGltns adhesives with different DSs. The gelation time increased with an increase in DS. The viscosities of Org and C8-ApGltn solutions were measured using a viscometer to clarify these phenomena. As shown in **Figure 3b** and **Figure S1**, the viscosity of the stC8 (H) solution was 6-fold higher than that of the asyC8 (H) solution, indicating that the aggregation property of the stC8 group was higher than that of asyC8. However, the viscosity of the 4S-PEG solution was 6.45 mPa·s. These results indicated a correlation between gelation time and viscosity of C8-ApGltns solutions (**Figure 3c**), suggesting that reaction kinetics between ApGltn and 4S-PEG was slower by inducing the less opportunity to react when the viscosity of ApGltn solution became high.

3.3. Swelling ratio

The swelling ratios of the adhesive hydrogels were evaluated using Org/stC8(L)/asyC8(L)/syC8(L)-ApGltns cured within 5 s. Swelling ratios of Org- and C8-ApGltns adhesive hydrogels increased up to 5 h and reached equilibrium within 24 h.

The swelling ratios of C8-ApGltns adhesive hydrogels were lower than that of the Org-ApGltn adhesive hydrogel (**Figure 3d**, **Figure S2**). This is because the C8-ApGltns adhesive hydrogels exhibited additional physical crosslinking derived from the straight/branched C8 groups. Among the C8-ApGltns adhesive hydrogels, the swelling ratio of the stC8-ApGltn adhesive hydrogel was lower than that of the asyC8/syC8-ApGltns adhesive hydrogel, indicating that the length of the main chain of the C8 group played a key role in decreasing the swelling ratios. The swelling ratio is determined by the osmotic pressure owing to differences in the polymer concentration and elastic pressure of the hydrogel network [27]. Although the polymer concentrations of the Org- and C8-ApGltns adhesive hydrogels were similar, the elastic pressure increased for the formation of physical crosslinking when the hydrophobic groups were introduced, resulting in a lower swelling ratio. In addition, the strength of hydrophobic interactions varies depending on the molecular structure, and the aggregation properties are different [28]. The swelling properties of the C8-ApGltns adhesive hydrogels were determined by the degree of physical crosslinking.

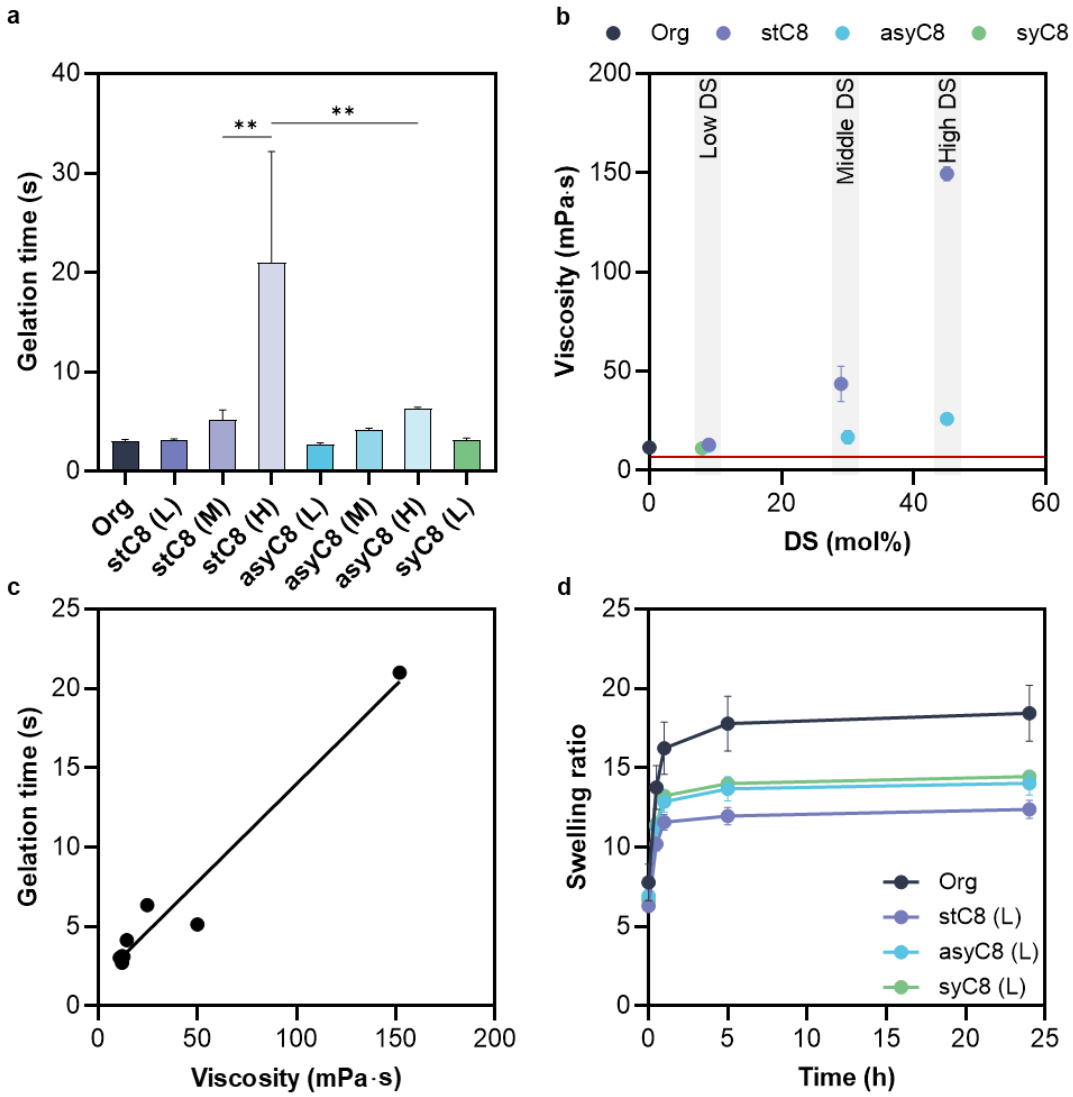

Figure 3. Physico-chemical properties of C8-ApGltns adhesives (**$p < 0.01$ using one-way ANOVA). a) Gelation time of Org/stC8/asyC8/syC8-ApGtlns adhesives. b) Viscosities of C8-ApGltns solutions with different DS. The red line indicates the viscosity of the 4S-PEG solution. c) Relation of viscosity of C8-ApGltn solution and their gelation time. d) Swelling behavior of Org- and C8-ApGltns adhesive hydrogels.

3.4. Rheological and mechanical properties of C8-ApGltns adhesive hydrogels

The rheological properties were evaluated to clarify the effect of the branched structures of the C8 groups on the modulus of the C8-ApGltns adhesive hydrogels (**Figure 4a-c**). This rheological measurement was performed to evaluate the viscoelasticity of completely formed hydrogels. We measured the shear strain from 0.01 to 100% to determine the LVE region (**Figure 4a**). From the results of the shear strain measurements, the strain ranged from 0.01-10%, indicating that these adhesive hydrogels were LVE in that range. Therefore, we measured the angular frequency of the Org- and C8-ApGltns adhesive hydrogels at a strain of 1%. From the angular frequency measurement, the G' of the Org- and C8-ApGltns adhesive hydrogels showed a plateau in the frequency ranging from 1 to 100 rad/s, indicating that these adhesive hydrogels had no dependence on frequency **(Figure 4b)**. G' of all C8-ApGltns adhesive hydrogels was larger than that of Org-ApGltn adhesive hydrogel (**Figure 4c**), meaning that straight/branched C8 groups in C8-ApGltns adhesive hydrogels contributed to the formation of physical crosslinking. Among three C8-ApGltns adhesive hydrogels, syC8(L) had the highest G', meaning that syC8 adhesive hydrogel was hard and strong against external force by storing the energy in the gel network. In addition, the G" value of stC8(L) was higher than that of syC8(L) and asyC8(L) (Figure 4b). This means that stC8 was weaker against external forces

because of its weak hydrogel network, which was prone to not storing energy.

The bulk strength of the Org/stC8(L)/asyC8(L)/syC8(L)-ApGltns adhesive hydrogel was evaluated using tensile strength measurements. As shown in Figure 4d, the stress-strain curves of each adhesive hydrogel revealed that these adhesive hydrogels were elastic materials. No significant differences in the maximum strain were observed among the Org/stC8(L)/asyC8(L)/syC8-ApGltns adhesive hydrogels (Figure S3c). In contrast, the maximum stress of syC8(L) was significantly higher than Org/ stC8(L)/asyC8(L)-ApGltns adhesive hydrogels. In addition, Young's modulus of the stC8(L)/asyC8(L)/syC8(L)-ApGltns adhesive hydrogels was 2-fold higher than that of the Org-ApGltn adhesive hydrogel (Figure 4e), indicating that the hydrogel network elasticity became stronger owing to the increase in physical crosslinking. As with the rheological measurement, syC8(L) showed the highest young's modulus. In comparison to straight chains, the gel network is more uniform due to that the shorter the main chain of the branch, the weaker the hydrophobic interaction, which is indicated to result in high storage modulus and Young's modulus.

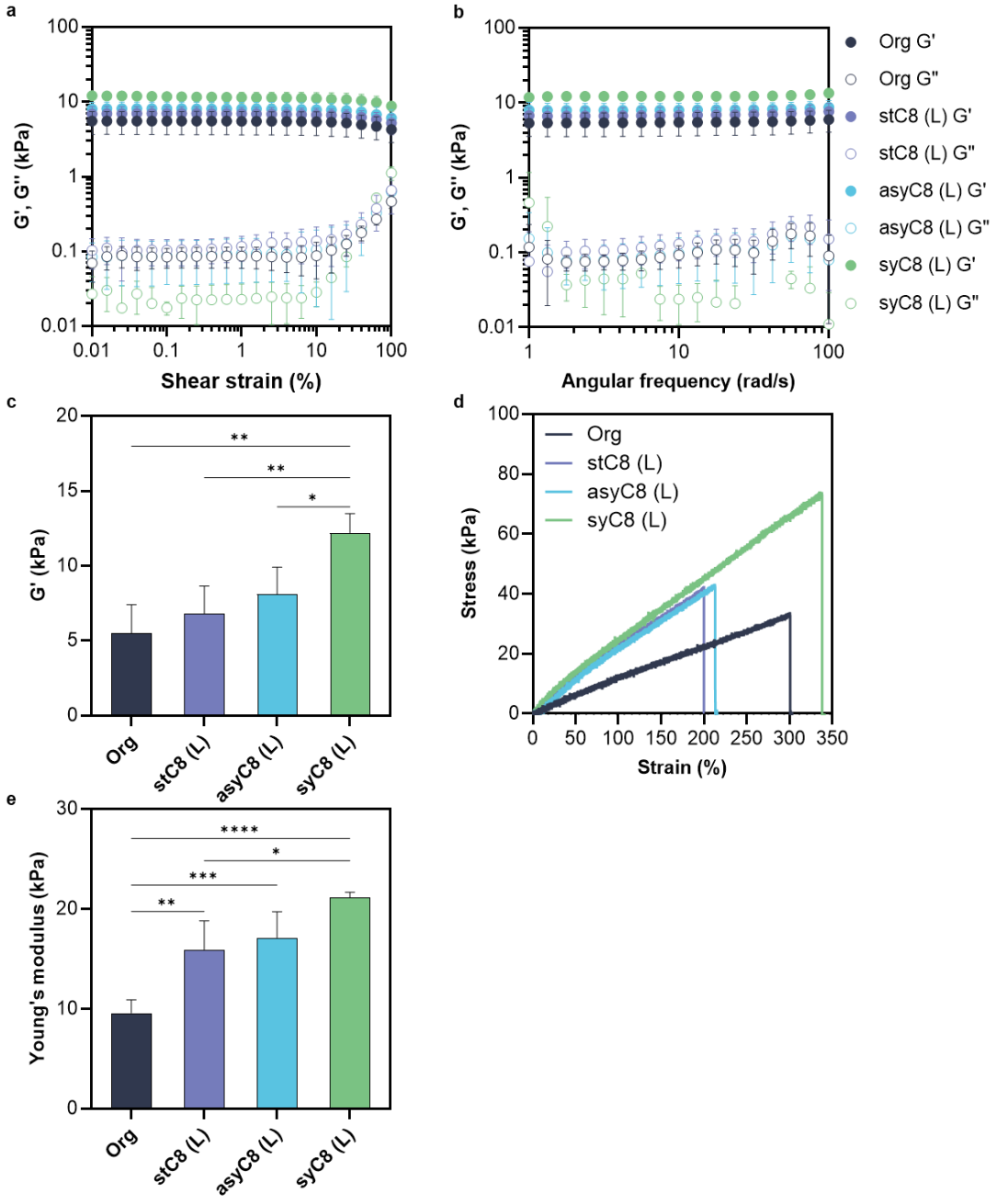

Figure 4. Rheological properties and tensile strength of C8-ApGltns adhesives. a) Shear strain dependency of G' and G". b) Angular frequency dependence of G' and G". c) Storage modulus of Org/stC8/asyC8/syC8-ApGtlns hydrogels at 10 rad/s, 1%. d) Stress-strain curve. e) Young's modulus. (*$p < 0.05$, **$p < 0.01$, ***$p < 0.001$, ****$p < 0.0001$ using one-way ANOVA)

3.5. Burst strength measurement

The burst strengths of the Org/stC8/asyC8-ApGltns adhesives and commercial Fibrin were measured using a collagen casing as the adherend. stC8/asyC8-ApGltns adhesives showed a lower burst strength when their DS increased (**Figure 5a**). This indicated that stC8/asyC8-ApGltns with low DS were mixed more uniformly with 4S-PEG because of their low viscosity. In contrast, the asyC8/syC8-ApGltn adhesives exhibited higher burst strength than the stC8-ApGltn adhesives at any DS and their burst strength were twice as high as those of Fibrin. We also analyzed the quantitative data of the destruction mode, such as the peeling or fracture of adhesives, after the application of adhesives to collagen casings to discuss these behaviors (**Figure 5b**). **Figure 5c** shows the destruction mode of each adhesive after burst strength measurements. The frequency of peeling increased at higher DS of the stC8-ApGltn adhesive, indicating that the interfacial adhesion strength weakened with an increase in DS. In contrast, the asyC8-ApGltn adhesive showed fracture behavior at any DS. This was because asyC8 contributed to hydrophobic interaction/interpenetration with collagen casing rather than self-aggregation because of its higher flexibility compared to stC8, while syC8(L) also showed high burst strength similar to asyC8(L). However, the mode of destruction of syC8(L) was different from that of asyC8(L) (**Figure 5c**). syC8(L) had a higher storage modulus than asyC8(L) (**Figure**

4a,b), indicating that the bulk strength of syC8(L) was higher than that of asyC8(L). It has been reported that the critical micelle concentration of surfactants with linear alkyl groups is lower than that of surfactants with branched alkyl groups [28], indicating that stC8 induces stronger aggregation than asyC8 or syC8. While, Fibrin showed the lowest burst strength with high peeling ratio, meaning interfacial strength between Fibrin and collagen casings was low. As shown in Figure 6, tissue adhesion of straight/branched alkyl group-modified ApGltns adhesives may be governed by the balance among inner aggregation (bulk strength), interfacial interaction (interfacial adhesive strength/hydrophobicity) and Young's modulus (elasticity). AsyC8(L)-ApGltn adhesive with middle inner aggregation properties, middle interfacial interaction properties and middle Young's modulus, results in the high burst strength (Figure 5a). While, syC8(L)-ApGltn adhesive may have low interfacial interaction properties, but has high bulk strength and Young's modulus, results in the high burst strength (Figure 5a).

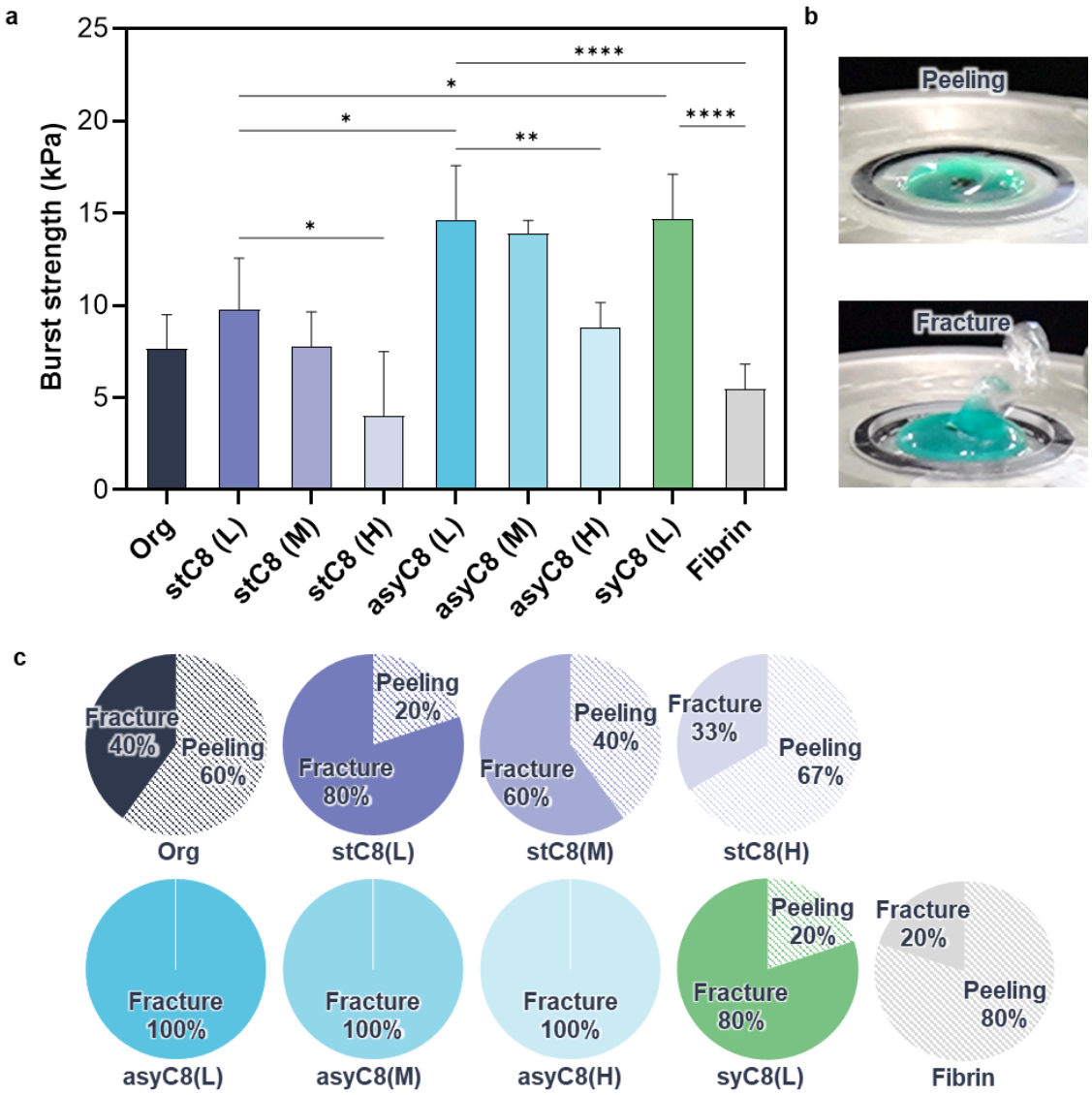

Figure 5. Burst strength of C8-ApGltns adhesives and Fibrin applied on collagen casing. a) Burst strength of Org/stC8/asyC8/syC8-ApGtlns adhesives with different DS and Fibrin. b) Destruction mode during burst strength measurement. c) Ratios of destruction mode of Org/stC8/asyC8/syC8-ApGtlns adhesives and Fibrin. (*$p < 0.05$, **$p < 0.01$ using one-way ANOVA)

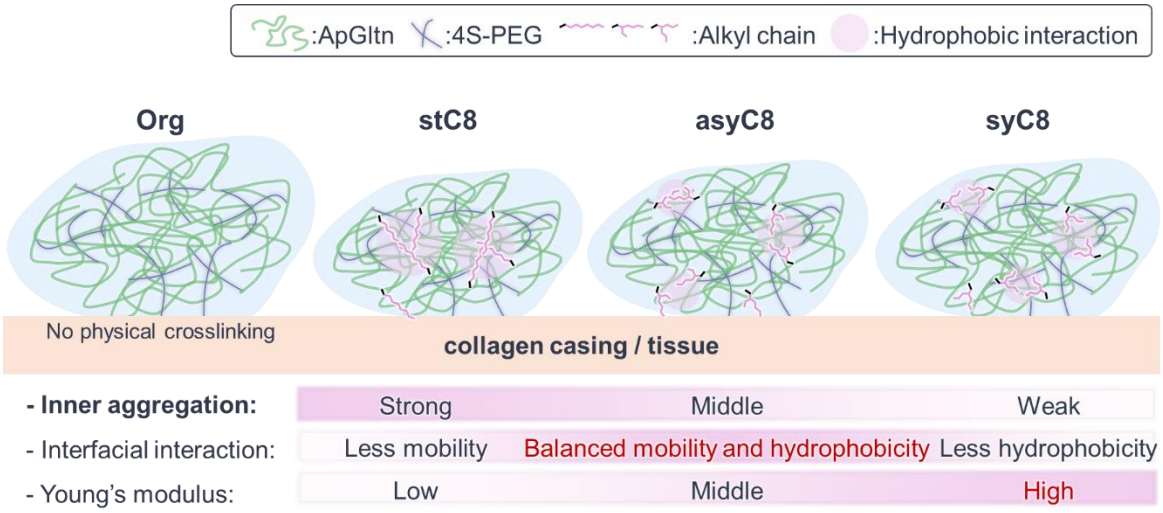

Figure 6. Tissue adhesion mechanisms of straight/branched alkyl groups-modified-ApGltns adhesives.

3.6. Enzymatic degradation study

The enzymatic degradability of the adhesive hydrogels was evaluated by immersion in a collagenase solution. All Org- and C8-ApGltns adhesive hydrogels were enzymatically degraded within 24 h (**Figure S5**). The weight remaining decreased with increasing immersion time. Among all the adhesive hydrogels examined, the Org-ApGltn adhesive hydrogel degraded rapidly. However, the stC8(L)/asyC8(L)-ApGltns adhesive hydrogels showed the slowest degradation rate among the C8-ApGltns adhesive hydrogels, indicating that their swelling ratio was lower than that of Org/syC8(L)-ApGltns adhesives, limiting the interpenetration of collagenase into the adhesive hydrogel matrix. All adhesive hydrogels can be enzymatically degraded in a similar process in vivo because the matrix metalloproteases (MMP)-2 and -9 selected from the cells during the wound healing process [29] facilitate the decomposition of gelatin from specific amino acid sequences such as Gly Pro-Gln-Gly Ile-Ala-Gly Gln [13]. The hydrolysis of the ester bond in 4S-PEG is believed to play a significant role in the degradation process of adhesive hydrogels. However, in this case, no decrease in mass was observed after 24 hours when swelling ratio was evaluated (**Figure 3c**), suggesting that the gelatin was cleaved by enzymes.

3.7. *Cytocompatibility*

The cytocompatibility of each Org or C8-ApGltn adhesive was evaluated according to ISO10993-5 and 10993-12 using an extraction medium. In this experiment, we used adhesive hydrogels from C8-ApGltns with a low DS because of their high burst strength (**Figure 5a**). Extraction media from all adhesive hydrogels showed over 80% cell viability compared to that of the control group (**Figure 7a**), indicating that these adhesives had good cytocompatibility. We also observed the cell morphology after staining with DAPI and FITC-phalloidin (**Figure 7b**). There were no significant differences between the Org and C8-ApGltns adhesive hydrogels and the control groups. These results suggested that straight/branched C8-ApGltns did not affect cell viability or morphology. Therefore, C8-ApGltns adhesives with a low DS do not hinder tissue regeneration when applied to wounds.

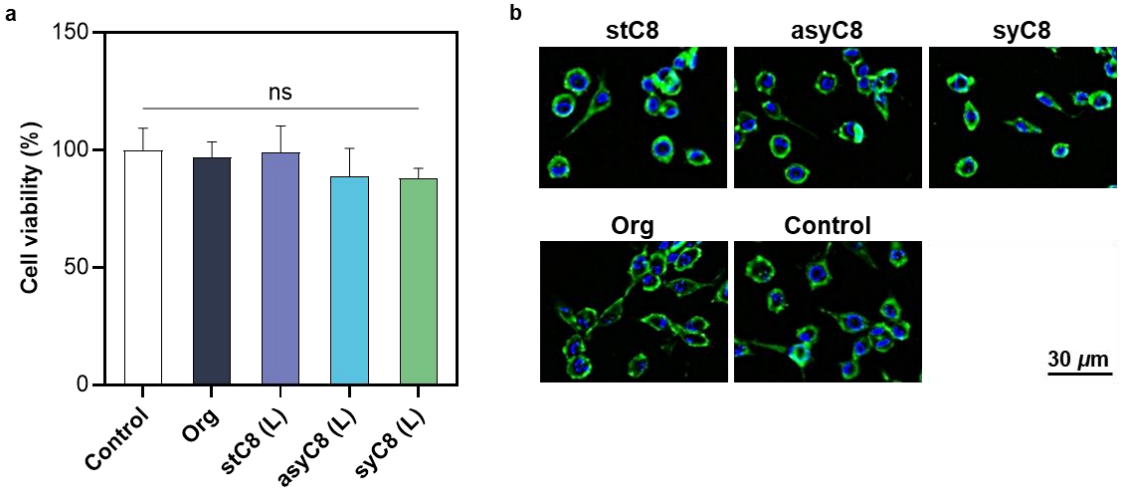

Figure 7. Cytocompatibility test. a) Viability of L929 cultured in extracted medium (ns = not significant using one-way ANOVA). b) Immunofluorescence images.

3.8. Subcutaneous implantation

The in vivo biodegradation behavior of Org and C8-ApGltns adhesives was evaluated using subcutaneous implantation of disk-shaped adhesive hydrogels on the backs of rats for up to 56 days (**Figure 8**). After implantation for 7 days, the Org-ApGltn adhesive hydrogel swelled in the subcutaneous tissue compared to the other adhesive hydrogels, similar to the in vitro results (**Figure 3d**). All adhesive hydrogels became smaller and thinner after implantation for 14 days, indicating that the degradation process had proceeded. Finally, all the adhesive hydrogels almost completely disappeared within 56 days. HE staining revealed that the surrounding tissue at the implant site infiltrated the adhesive hydrogel as the duration of the implantation period increased. This suggested that the adhesive hydrogels functioned as scaffolds to facilitate tissue regeneration. Gelatin is a denatured collagen with a cell adhesion peptide sequence of Arg-Gly-Asp [30]. Cells in the surrounding tissues recognized the cell adhesion sequence to infiltrate the adhesive hydrogels. MMPs are expressed in endothelial cells, fibroblasts, neutrophils, and macrophages during wound healing [31-33]. Therefore, specific amino acid sequences in C8-ApGltns adhesive hydrogels are cleaved and enzymatically degraded by MMPs, such as MMP-2 or -9 secreted from these cells [34]. In addition, 4S-PEG decomposes through ester hydrolysis and ether oxidative decomposition [17, 35, 36]. We

previously reported that the degradation speed of hydrophobically modified ApGltn adhesive hydrogels in rat subcutaneous tissue was relatively slow compared to that of the Org-ApGltn adhesive hydrogel owing to its additional physical crosslinking by hydrophobic groups [13, 17, 37]. However, we did not observe such differences in this study because of the short alkyl chain (C8) and low DS (~10 mol%). Additionally, we did not observe any foreign body reaction, including the deposition of collagen-rich areas, indicating that the C8-ApGltns adhesive hydrogels are biodegradable and have excellent biocompatibility.

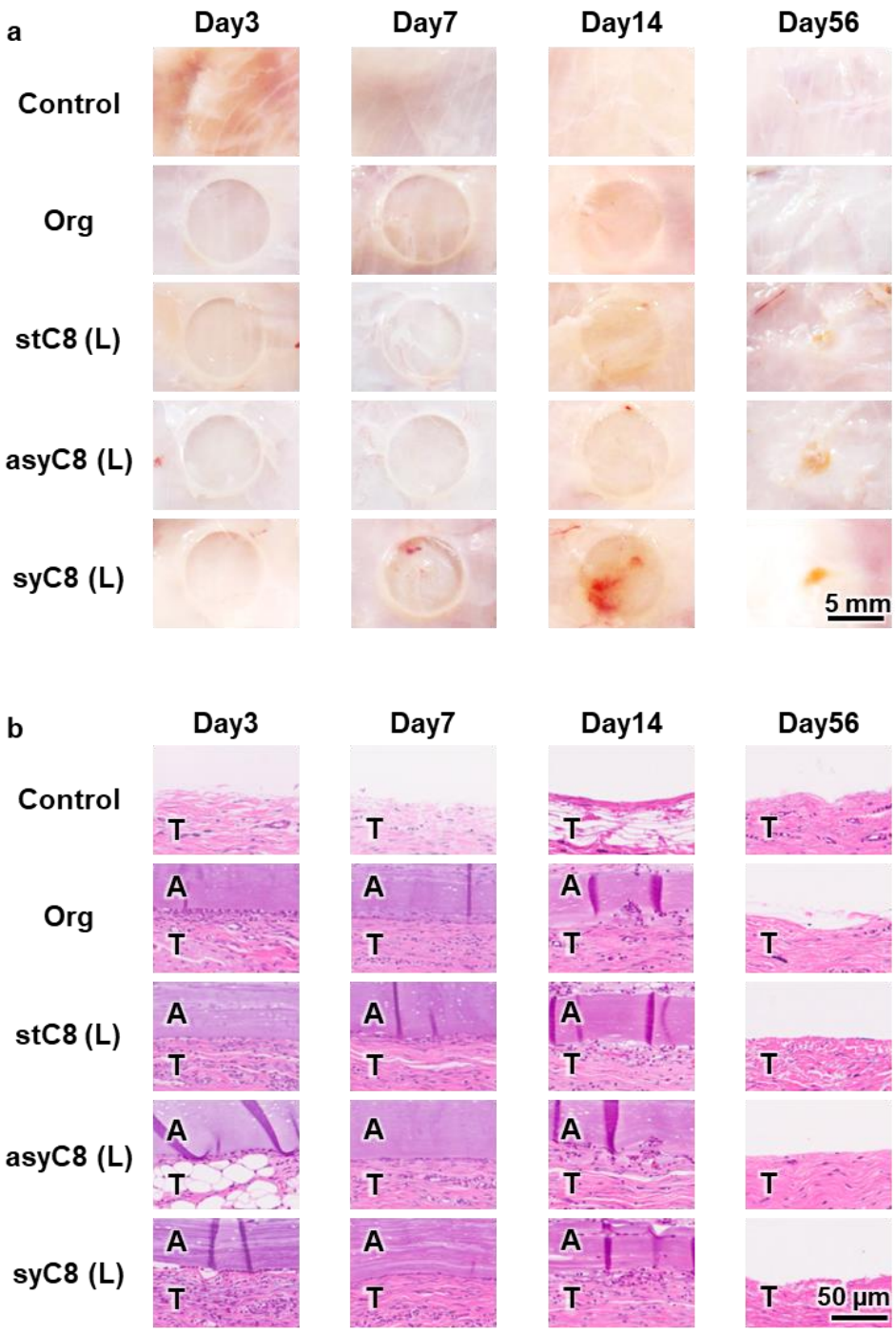

Figure 8. a) Biodegradability of C8-ApGltn adhesive hydrogels after implantation in rat subcutaneous tissue for various periods. b) Tissues stained by hematoxylin and eosin (HE) extracted for each period. A and T in HE-staining images represent Adhesive and Tissue.

4. Conclusion

The adhesion properties and biocompatibility of the tissue adhesives composed of straight/branched C8-ApGltns and 4S-PEG were evaluated. Branched alkyl groups (asyC8/syC8) contributed to a higher burst strength than straight alkyl groups (stC8). The high burst strength of asyC8-ApGltn adhesive came from interfacial strength, achieved by having adequate hydrophobicity to interact with tissues and mobility of the alkyl groups from their self-aggregation property. In contrast, the syC8-ApGltn adhesive hydrogel had the highest bulk strength, as revealed by rheological measurements. Additionally, the stC8/asyC8/syC8-ApGltns adhesive exhibited excellent cytocompatibility and completely degraded subcutaneously within 56 days without severe inflammation. The structural comparison of alkyl groups in this study will provide new insight into the role of hydrophobic modification on tissue adhesion.

Data Availability

The authors declare that all data supporting the findings of this study are available in the paper and the associated Supporting Information.

Conflicts of Interest

The authors have no competing interests to declare.

Acknowledgements

This work was financially supported in part by the Japan Society for the Promotion of Science (JSPS KAKENHI) Grant-in-Aid for JSPS Fellows (grant nos. 24KJ0500 and 22KJ0418) and JSPS KAKENHI (grant nos. 23K25216, 23K26411, 24K21677, and 24K22399).

Appendix a. Supplementary Data

Supplementary data related to this article can be found at

References

[1] G.M. Taboada, K. Yang, M.J.N. Pereira, S.S. Liu, Y. Hu, J.M. Karp, N. Artzi, Y. Lee, Overcoming the translational barriers of tissue adhesives, Nat. Rev. Mater. 5 (2020) 310–329. https://doi.org/10.1038/s41578-019-0171-7.

[2] A.I. Bochyńska, G. Hannink, P. Buma, D.W. Grijpma, Adhesion of tissue glues to different biological substrates, Polym. Adv. Technol. 28 (2017) 1294–1298. https://doi.org/10.1002/pat.3909.

[3] S.S. Bhatia, Ocular surface sealants and adhesives, Ocul. Surf. 4 (2006) 146–154. https://doi.org/10.1016/s1542-0124(12)70041-1.
[4] M.M. Joglekar, D.-J. Slebos, J. Leijten, J.K. Burgess, S.D. Pouwels, Crosslink bio-adhesives for bronchoscopic lung volume reduction: Current status and future direction, Eur. Respir. Rev. 30 (2021) 210142. https://doi.org/10.1183/16000617.0142-2021.
[5] W. Fürst, A. Banerjee, Release of glutaraldehyde from an albumin-glutaraldehyde tissue adhesive causes significant in vitro and in vivo toxicity, Ann. Thorac. Surg. 79 (2005) 1522–1528; discussion 1529. https://doi.org/10.1016/j.athoracsur.2004.11.054.
[6] S. Nam, D. Mooney, Polymeric tissue adhesives, Chem. Rev. 121 (2021) 11336–11384. https://doi.org/10.1021/acs.chemrev.0c00798.
[7] C. Li, Y. Qian, X. Zhang, R. Wang, Robust-adhesion and high-mechanical strength hydrogel for efficient wet tissue adhesion, J. Mater. Chem. B. 13 (2025) 2469–2479. https://doi.org/10.1039/d4tb02357a.
[8] T. Sakai, T. Matsunaga, Y. Yamamoto, C. Ito, R. Yoshida, S. Suzuki, N. Sasaki, M. Shibayama, U.-i. Chung, Design and fabrication of a high-strength hydrogel with ideally homogeneous network structure from tetrahedron-like macromonomers, Macromolecules. 41 (2008) 5379–5384. https://doi.org/10.1021/ma800476x.
[9] K. Ito, Novel Cross-Linking Concept of Polymer Network, Novel Cross-Linking Concept of Polymer Network: Synthesis, structure, and properties of slide-ring gels with freely movable junctions, Polym. J. 39 (2007) 489–499. https://doi.org/10.1295/polymj.PJ2006239.
[10] R. Michel, L. Corté, Hydrogel–tissue adhesion by particle bridging: Sensitivity to interfacial wetting and tissue composition, Soft Matter. 20 (2024) 5122–5133. https://doi.org/10.1039/d4sm00287c.
[11] X. Yan, H. Huang, A.M. Bakry, W. Wu, X. Liu, F. Liu, Advances in enhancing the mechanical properties of biopolymer hydrogels via multi-strategic approaches, Int. J. Biol. Macromol. 272 (2024) 132583. https://doi.org/10.1016/j.ijbiomac.2024.132583.
[12] R. Mizuta, T. Taguchi, Enhanced sealing by hydrophobic modification of Alaska pollock-derived gelatin-based surgical sealants for the treatment of pulmonary air leaks, Macromol. Biosci. 17 (2017). https://doi.org/10.1002/mabi.201600349.
[13] Y. Mizuno, R. Mizuta, M. Hashizume, T. Taguchi, Enhanced sealing strength of a hydrophobically-modified Alaska pollock gelatin-based sealant, Biomater Sci-Uk. 5 (2017) 982–989. https://doi.org/10.1039/c6bm00829a.
[14] F. Xavier Perrin, T.B. Viet Nguyen, A. Margaillan, Linear and branched alkyl substituted octakis(dimethylsiloxy)octasilsesquioxanes: WAXS and thermal properties, Eur. Polym. J. 47 (2011) 1370–1382. https://doi.org/10.1016/j.eurpolymj.2011.04.004.
[15] G.S. Parks, H.M. Huffman, S.B. Thomas, Thermal data on organic compounds. VI. The heat

capacities, entropies and free energies of some saturated, non-benzenoid HYDROCARBONS1, J. Am. Chem. Soc. 52 (1930) 1032–1041. https://doi.org/10.1021/ja01366a030.
[16] C. Fong, T.L. Greaves, T.W. Healy, C.J. Drummond, The effect of structural modifications on the solution and interfacial properties of straight and branched aliphatic alcohols: The role of hydrophobic effects, J. Colloid Interface Sci. 449 (2015) 364–372. https://doi.org/10.1016/j.jcis.2015.01.045.
[17] H. Komatsu, S. Watanabe, S. Ito, K. Nagasaka, A. Nishiguchi, T. Taguchi, Improved swelling property of tissue adhesive hydrogels based on α - cyclodextrin/decyl group - modified Alaska Pollock gelatin inclusion complexes, Macromol. Biosci. 23 (2023) e2300097. https://doi.org/10.1002/mabi.202300097.
[18] R. Mizuta, Y. Mizuno, X. Chen, Y. Kurihara, T. Taguchi, Evaluation of an octyl group-modified Alaska pollock gelatin-based surgical sealant for prevention of postoperative adhesion, Acta Biomater. 121 (2021) 328–338. https://doi.org/10.1016/j.actbio.2020.12.025.
[19] A.F. Habeeb, Determination of free amino groups in proteins by trinitrobenzenesulfonic acid, Anal. Biochem. 14 (1966) 328–336. https://doi.org/10.1016/0003-2697(66)90275-2.
[20] J. Adler-Nissen, Determination of the degree of hydrolysis of food protein hydrolysates by trinitrobenzenesulfonic acid, J. Agric. Food Chem. 27 (1979) 1256–1262. https://doi.org/10.1021/jf60226a042.
[21] K. Nagasaka, S. Watanabe, S. Ito, H. Ichimaru, A. Nishiguchi, H. Otsuka, T. Taguchi, Enhanced burst strength of catechol groups-modified Alaska pollock-derived gelatin-based surgical adhesive, Colloids Surf. B Biointerfaces. 220 (2022) 112946. https://doi.org/10.1016/j.colsurfb.2022.112946.
[22] T.M. Shazly, N. Artzi, F. Boehning, E.R. Edelman, Viscoelastic adhesive mechanics of aldehyde-mediated soft tissue sealants, Biomaterials. 29 (2008) 4584–4591. https://doi.org/10.1016/j.biomaterials.2008.08.032.
[23] S.-H. Hyon, N. Nakajima, H. Sugai, K. Matsumura, Low cytotoxic tissue adhesive based on oxidized dextran and epsilon-poly-l-lysine, J. Biomed. Mater. Res. A. 102 (2014) 2511–2520. https://doi.org/10.1002/jbm.a.34923.
[24] Y. Mizuno, T. Taguchi, Promotion of Cell Migration into a hydrophobically modified Alaska Pollock Gelatin-Based Hydrogel, Macromol. Biosci. 19 (2019) e1900083. https://doi.org/10.1002/mabi.201900083.
[25] H. Ichimaru, T. Taguchi, Improved tissue adhesion property of a hydrophobically modified Alaska pollock derived gelatin sheet by UV treatment, Int. J. Biol. Macromol. 172 (2021) 580–588. https://doi.org/10.1016/j.ijbiomac.2021.01.085.
[26] J. Kim, H. Keum, H. Albadawi, Z. Zhang, E.H. Graf, E. Cevik, R. Oklu, Multi-functional biomaterial for the treatment and prevention of central line-associated bloodstream infections,

Adv. Mater. 36 (2024) e2405805. https://doi.org/10.1002/adma.202405805.
[27] H. Kamata, K. Kushiro, M. Takai, U.-I. Chung, T. Sakai, Non-osmotic hydrogels: A rational strategy for safely degradable hydrogels, Angew. Chem. Int Ed Engl. 55 (2016) 9282–9286. https://doi.org/10.1002/anie.201602610.
[28] S. Alexander, G.N. Smith, C. James, S.E. Rogers, F. Guittard, M. Sagisaka, J. Eastoe, Low-surface energy surfactants with branched hydrocarbon architectures, Langmuir. 30 (2014) 3413–3421. https://doi.org/10.1021/la500332s.
[29] P.-H. Wang, B.-S. Huang, H.-C. Horng, C.-C. Yeh, Y.-J. Chen, Wound healing, J. Chin. Med. Assoc. 81 (2018) 94–101. https://doi.org/10.1016/j.jcma.2017.11.002.
[30] I.W. Hamley, Small bioactive peptides for biomaterials design and therapeutics, Chem. Rev. 117 (2017) 14015–14041. https://doi.org/10.1021/acs.chemrev.7b00522.
[31] S. Mondal, N. Adhikari, S. Banerjee, S.A. Amin, T. Jha, Matrix metalloproteinase-9 (MMP-9) and its inhibitors in cancer: A minireview, Eur. J. Med. Chem. 194 (2020) 112260. https://doi.org/10.1016/j.ejmech.2020.112260.
[32] A. Salajegheh, Matrix metalloproteinase 2 (MMP2), in: A. Salajegheh (Ed.), Angiogenesis in Health, Disease and Malignancy, Springer International Publishing, Cham, 2016, pp. 203–208. https://doi.org/10.1007/978-3-319-28140-7_31.
[33] T. Klein, R. Bischoff, Physiology and pathophysiology of matrix metalloproteases, Amino Acids. 41 (2011) 271–290. https://doi.org/10.1007/s00726-010-0689-x.
[34] J.L. Seltzer, K.T. Akers, H. Weingarten, G.A. Grant, D.W. McCourt, A.Z. Eisen, Cleavage specificity of human skin type IV collagenase (gelatinase). Identification of cleavage sites in type I gelatin, with confirmation using synthetic peptides, J. Biol. Chem. 265 (1990) 20409–20413. https://doi.org/10.1016/S0021-9258(17)30519-7.
[35] Y. Mizuno, S. Watanabe, M. Katano, T. Yanagihara, N. Maki, Y. Sato, T. Taguchi, Comparative study of hydrophobically modified gelatin-based sealant with commercially available sealants, J. Biomed. Mater. Res. A. 110 (2022) 909–915. https://doi.org/10.1002/jbm.a.37339.
[36] M.B. Browning, S.N. Cereceres, P.T. Luong, E.M. Cosgriff-Hernandez, Determination of the in vivo degradation mechanism of PEGDA hydrogels, J. Biomed. Mater. Res. A. 102 (2014) 4244–4251. https://doi.org/10.1002/jbm.a.35096.
[37] R. Mizuta, T. Ito, T. Taguchi, Effect of alkyl chain length on the interfacial strength of surgical sealants composed of hydrophobically-modified Alaska-pollock-derived gelatins and poly(ethylene)glycol-based four-armed crosslinker, Colloids Surf. B Biointerfaces. 146 (2016) 212–220. https://doi.org/10.1016/j.colsurfb.2016.06.017.

The effect of branched structures of alkyl groups on tissue adhesiveness and biocompatibility of alkyl groups-modified Alaska pollock gelatin-based adhesives

Satsuki Minamisakamoto[1,2], Hiyori Komatsu[1,2], Shiharu Watanabe[2], Shima Ito[1,2], Hatsune Nishino[2,3], Tetsushi Taguchi[1,2]*

[1]Graduate School of Science and Technology, Degree Programs in Pure and Applied Sciences, University of Tsukuba, 1-1-1 Tennodai, Tsukuba, Ibaraki 305-8577, Japan

[2]Biomaterials field, Research Center for Macromolecules and Biomaterials, National Institute for Materials Science, 1-1 Namiki, Tsukuba, Ibaraki 305-0044, Japan

[3]College of Engineering Science, School of Science and Engineering, University of Tsukuba, 1-1-1 Tennodai, Tsukuba, Ibaraki 305-8577, Japan

Correspondence and requests for materials should be addressed to T. Taguchi. (email: TAGUCHI.Tetsushi@nims.go.jp)

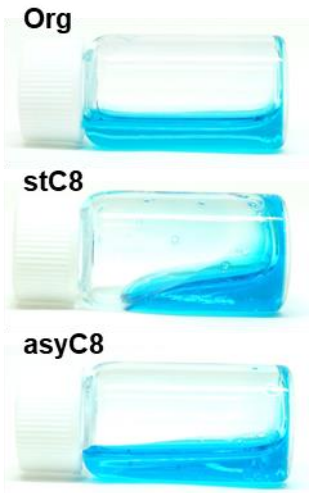

Figure S1. Appearance of Org/stC8/asyC8-ApGltn solution (15% (w/v)). DS of stC8 or asyC8-ApGltn were 45.3(H) and 44.5(H) mol%, respectively.

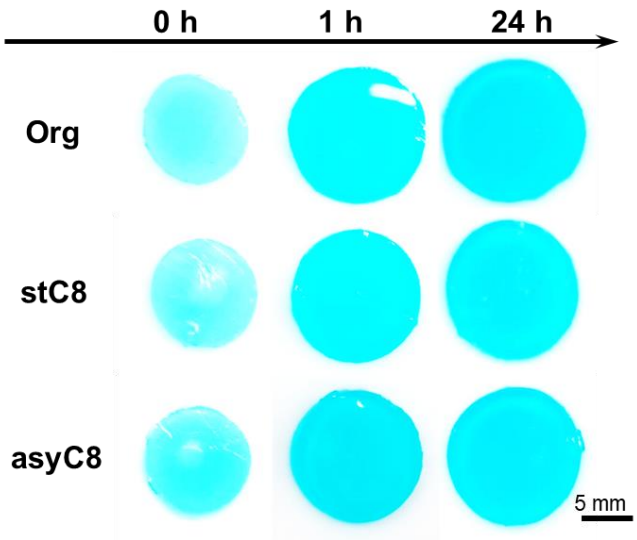

Figure S2. Appearance of Org/stC8/asyC8-ApGltn adhesive hydrogels before and after immersed in D-PBS. DS of stC8/asyC8-ApGltns were 9.1(L) and 9.4(L) mol%, respectively.

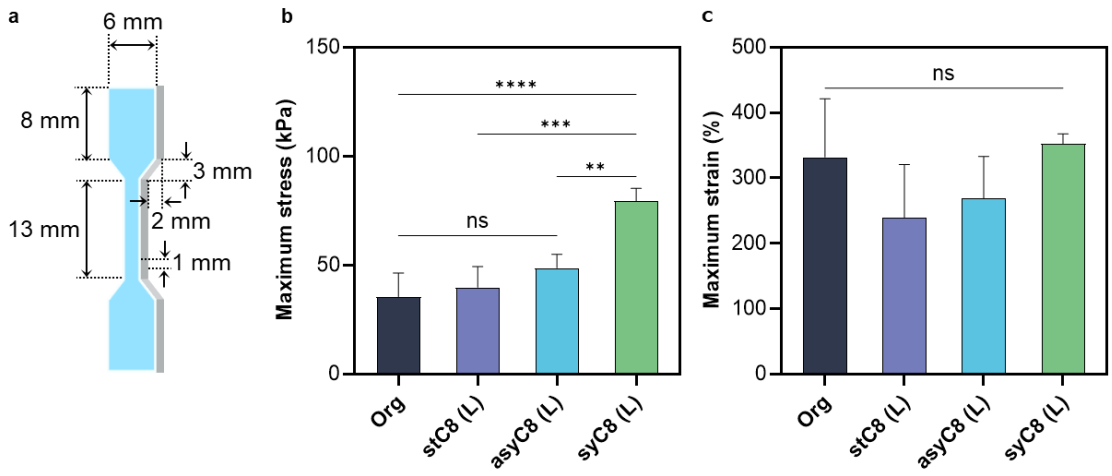

Figure S3. Tensile strength of cured Org/stC8(L)/asyC8(L)syC8(L)-ApGltn adhesives. a) Dumbbell-shape adhesive hydrogels for tensile strength measurement. b) Maximum stress. c) Maximum strain. (*$p < 0.05$, **$p < 0.01$, ***$p < 0.001$, ns = not significant using one-way ANOVA)

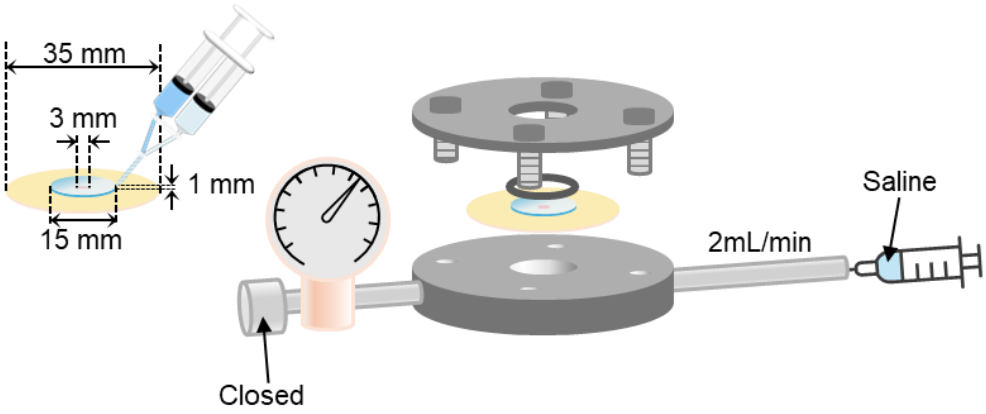

Figure S4. Measurement of burst strength using ASTM 2392-04.

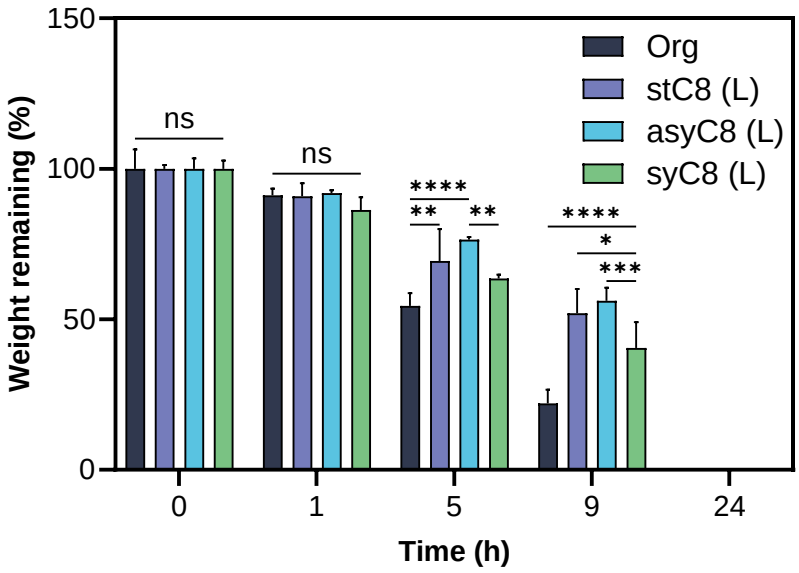

Figure S5. Enzymatic degradability of Org/stC8/asyC8/syC8-ApGltn adhesive hydrogels in a collagenase solution. (*$p < 0.05$, **$p < 0.01$, ***$p < 0.001$, ****$p < 0.0001$, ns = no significant using two-way ANOVA)

Declaration of interests

☒The authors declare that they have no known competing financial interests or personal relationships that could have appeared to influence the work reported in this paper.

☐The authors declare the following financial interests/personal relationships which may be considered as potential competing interests: